

Unique Fermi surfaces with quasi-one-dimensional character in CeRh_3B_2 and LaRh_3B_2

This article has been downloaded from IOPscience. Please scroll down to see the full text article.

2003 J. Phys.: Condens. Matter 15 L721

(<http://iopscience.iop.org/0953-8984/15/46/L02>)

View [the table of contents for this issue](#), or go to the [journal homepage](#) for more

Download details:

IP Address: 171.66.16.125

The article was downloaded on 19/05/2010 at 17:44

Please note that [terms and conditions apply](#).

LETTER TO THE EDITOR

Unique Fermi surfaces with quasi-one-dimensional character in CeRh_3B_2 and LaRh_3B_2

T Okubo¹, M Yamada¹, A Thamizhavel¹, S Kirita¹, Y Inada^{1,5}, R Settai¹, H Harima², K Takegahara³, A Galatanu⁴, E Yamamoto⁴ and Y Ōnuki^{1,4}

¹ Graduate School of Science, Osaka University, Toyonaka, Osaka 560-0043, Japan

² The Institute of Scientific and Industrial Research, Osaka University, Ibaraki, Osaka 567-0047, Japan

³ Department of Materials Science and Technology, Hirosaki University, Hirosaki, Aomori 036-8561, Japan

⁴ Advance Science Research Centre, Japan Atomic Energy Research Institute, Tokai, Ibaraki 319-1195, Japan

Received 13 October 2003

Published 7 November 2003

Online at stacks.iop.org/JPhysCM/15/L721

Abstract

We have carried out de Haas–van Alphen (dHvA) experiments on a ferromagnet CeRh_3B_2 with an extremely high Curie temperature $T_C \simeq 120$ K and a non-4f reference compound LaRh_3B_2 . The dHvA data of LaRh_3B_2 are well explained by the results of energy band calculations. The topology of the Fermi surfaces in CeRh_3B_2 is found to be very similar to that of LaRh_3B_2 , possessing wavy but flat Fermi surfaces in the basal plane. Observation of a quasi-one-dimensional electronic state is the first such case in a rare earth compound.

In order to gain a deeper understanding of magnetic and superconducting properties in cerium and uranium compounds, it is essentially important to clarify the nature of the f electrons: namely whether they are itinerant or localized. This issue is closely related to the strongly correlated nature of conduction electrons, which hinders the conduction electrons to move freely due to the strong Coulomb repulsion, and consequently these electrons have tendency to localize. The strongly correlated electrons are thus found to behave in some cases like itinerant electrons and in other cases like localized electrons, depending on the temperature region and/or on the compound [1, 2].

CeRh_3B_2 , with the hexagonal structure of space group $P6/mmm$ (#191), has attracted a considerable interest due to its anomalous ferromagnetic properties [3–5]. The Curie temperature $T_C \simeq 120$ K is the highest value in the cerium compounds. Surprisingly the Curie temperature $T_C \simeq 120$ K is far above $T_C = 91$ K in GdRh_3B_2 . This means that $T_C \simeq 120$ K in

⁵ On leave from: Osaka University, Faculty of Education, Okayama University, 3-1-1 Tsushimanaka, Okayama 700-8530, Japan.

CeRh_3B_2 is two orders of magnitude higher than the magnetic ordering temperature expected from the de Gennes factor consideration. An ordered magnetic moment of $0.4 \mu_{\text{B}}/\text{Ce}$, which is oriented within the basal plane, is relatively small compared to the usual value of about $1 \mu_{\text{B}}/\text{Ce}$ [6].

The hexagonal crystal structure is anomalous. The c -value of 3.096 \AA at room temperature is very short, smaller than 3.41 \AA in α -Ce with valence close to $4+$, namely without $4f$ magnetism, while the a -value of 5.469 \AA is normal [7–9]. The temperature dependence of the lattice constants for LaRh_3B_2 , CeRh_3B_2 and a ferromagnet PrRh_3B_2 with $T_{\text{C}} = 2 \text{ K}$ indicates that both the a - and c -values of LaRh_3B_2 and PrRh_3B_2 monotonously decrease with decreasing temperature, while in CeRh_3B_2 the a -value increases below 300 K and consequently the c -value decreases steeply below 300 K . The quasi-one-dimensional character along the c -axis is enhanced at lower temperatures in CeRh_3B_2 .

From these experimental results it was suggested that ferromagnetism is not based on the $4f$ localized moment but an intermediate valence or even itinerant magnetism [3, 4, 9]. On the other hand, NMR, photoemission spectroscopy, x-ray absorption spectroscopy experiments as well as a La-substitution study indicated that there are no magnetic moments on the Rh and B sites and the magnetic moment is located on the Ce atom [10–13]. From a polarized neutron scattering study, it was clarified that the magnetic moment of the cerium ion is $\mu_{\text{Ce}} = \mu_{4f} + \mu_{5d} = 0.38 \mu_{\text{B}}$: the $4f$ magnetic moment $\mu_{4f} = +0.56 \mu_{\text{B}}$ and the non-negligible Ce $5d$ magnetic moment $\mu_{5d} = -0.18 \mu_{\text{B}}$ [14]. This value is in good agreement with the experimental value of $0.4 \mu_{\text{B}}$. Quite recently the ferromagnetism in CeRh_3B_2 has been theoretically discussed on the basis of a two-band model of which the basic ingredient is an uncorrelated dispersive band hybridized with a correlated and narrow band [15].

This letter reports the first experimental results of de Haas–van Alphen (dHvA) oscillations to clarify the Fermi surface property. These experiments on CeRh_3B_2 were not carried out previously mainly due to the poor quality of the single crystal sample. The experimental results on CeRh_3B_2 are compared to the dHvA results of a corresponding non- $4f$ reference compound LaRh_3B_2 and the theoretical results of full potential LAPW (FLAPW) band calculations of LaRh_3B_2 , indicating the existence of unique Fermi surfaces, namely wavy but flat Fermi surfaces in the basal plane.

Single crystals of CeRh_3B_2 and LaRh_3B_2 were grown by the Czochralski pulling method in a tetra-arc furnace. Starting materials were 99.9%-pure Ce and La, 99.99%-pure Rh and 99.99%-pure B. Ingots were about 3 mm in diameter and 40 mm in length, which were annealed at $900 \text{ }^\circ\text{C}$ in high vacuum of 10^{-10} Torr .

The residual resistivity ρ_0 and residual resistivity ratio ρ_{RT}/ρ_0 in CeRh_3B_2 were $\rho_0 = 2.0 \mu\Omega \text{ cm}$ and $\rho_{\text{RT}}/\rho_0 = 58$ for the current along $[10\bar{1}0]$. This indicates the best quality sample, as far as we know. The corresponding values of LaRh_3B_2 were $\rho_0 = 1.1 \mu\Omega \text{ cm}$ and $\rho_{\text{RT}}/\rho_0 = 89$. The dHvA experiments were done at high magnetic fields up to 170 kOe and low temperatures down to 30 mK . The dHvA voltage was obtained in the so-called 2ω detection of the field modulation method [1].

Figure 1 shows the typical dHvA oscillation in the field range from 120 to 169 kOe at 30 mK for $H \parallel [0001]$ (c -axis) and the corresponding fast Fourier transformation (FFT) spectrum of CeRh_3B_2 . We detected five kinds of fundamental branches, named α , β_1 , ε , β_2 and γ_2 , together with harmonics, where the dHvA frequency $F(=c\hbar/2\pi e)S_{\text{F}}$ is proportional to an extremal (maximum or minimum) cross-sectional area S_{F} of the Fermi surface. From the temperature dependence of the dHvA amplitude, we can determine the cyclotron effective mass m_{c}^* . The cyclotron mass is rather light, ranging from 0.3 to $3 m_0$.

Figure 2 shows the angular dependence of the dHvA frequency. Each branch is characterized as follows.

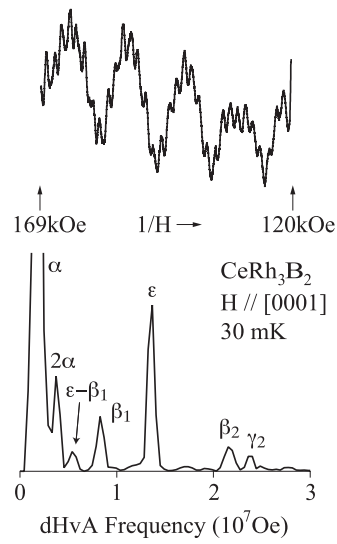


Figure 1. dHvA oscillation and its FFT spectrum for the field along [0001] in CeRh_3B_2 .

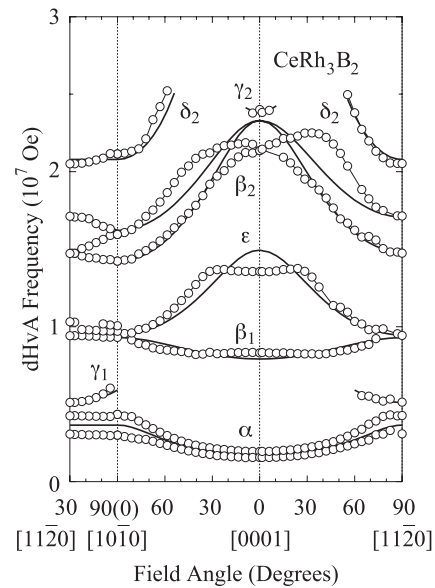


Figure 2. Angular dependence of the dHvA frequency in CeRh_3B_2 . Thick solid curves correspond to the Fermi surfaces shown in figures 4(f)–(j).

- (1) branch α : an ellipsoidal Fermi surface elongated along [0001], which is most likely split into two kinds of Fermi surfaces with up- and down-spin states;
- (2) branch β_1 : an approximately spherical Fermi surface;
- (3) branch ϵ : an ellipsoidal Fermi surface shrunken along [0001];
- (4) branch β_2 : three ellipsoidal Fermi surfaces;
- (5) branch δ_2 : a flat ellipsoidal Fermi surface.

The other branches, γ_1 and γ_2 , are detected in the basal plane and around [0001], respectively.

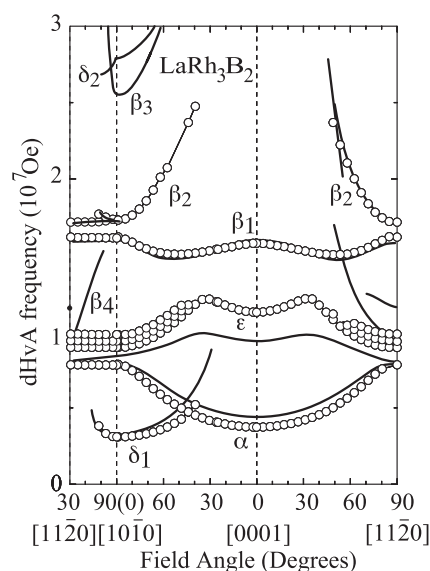


Figure 3. Angular dependence of the dHvA frequency in LaRh_3B_2 . Thick solid curves correspond to the theoretical Fermi surfaces.

We can estimate the topology of the corresponding Fermi surface, which is shown by thick solid curves in figure 2. The exact Fermi surface is discussed later on the basis of the Fermi surface of LaRh_3B_2 .

To understand the topology of the Fermi surface in CeRh_3B_2 , we have also carried out the same dHvA experiments for LaRh_3B_2 . We show in figure 3 the angular dependence of the dHvA frequency of LaRh_3B_2 . Branches α , β_1 and ε in LaRh_3B_2 are very similar to the corresponding branches in CeRh_3B_2 , although the absolute magnitude of the dHvA frequency is slightly different. The cyclotron mass of LaRh_3B_2 is in the range from 0.3 to 1.3 m_0 .

The solid curves in figure 3 indicate the theoretical results based on the FLAPW band calculations, which are in good agreement with the experimental results. The calculations were performed by modifying the local density approximation (LDA) for the exchange–correlation potential. We found that the slight modification of the LDA band structure is necessary to describe the experimental Fermi surfaces. The La 4f and La 5d levels were artificially shifted upward from the LDA levels by 0.2 and 0.1 Ryd, respectively. Such modifications were important to construct the previous Fermi surface study in LaB_6 [16] and YbAl_3 [17], for example. The lattice constants used for the calculations were $a = 5.480 \text{ \AA}$ and $c = 3.137 \text{ \AA}$ [7]. The density of states at the Fermi level is calculated as $7.37 \text{ mJ K}^{-2} \text{ mol}^{-1}$. The results of the band structure calculations, together with the method, will be published in a separated paper [18].

The theoretical Fermi surfaces are shown in figures 4(a)–(e), where bands 30 and 31 correspond to hole Fermi surfaces and bands 32–34 are due to compensated electron Fermi surfaces, indicating that LaRh_3B_2 is a compensated metal with equal volumes of electron and hole Fermi surfaces. It is noted that there exist two kinds of quasi-one-dimensional flat bands 32- and 33-electron Fermi surfaces. The dHvA branches named α , β_i , δ_i and ε are identified in the Fermi surfaces in figures 4(a)–(e). Theoretical orbits named β_3 , β_4 and δ_2 are, however, not detected experimentally most likely because of a small curvature factor of these orbits. Moreover, a quasi-one-dimensional band 32-electron Fermi surface cannot be detected in the dHvA experiment because of no closed orbits.

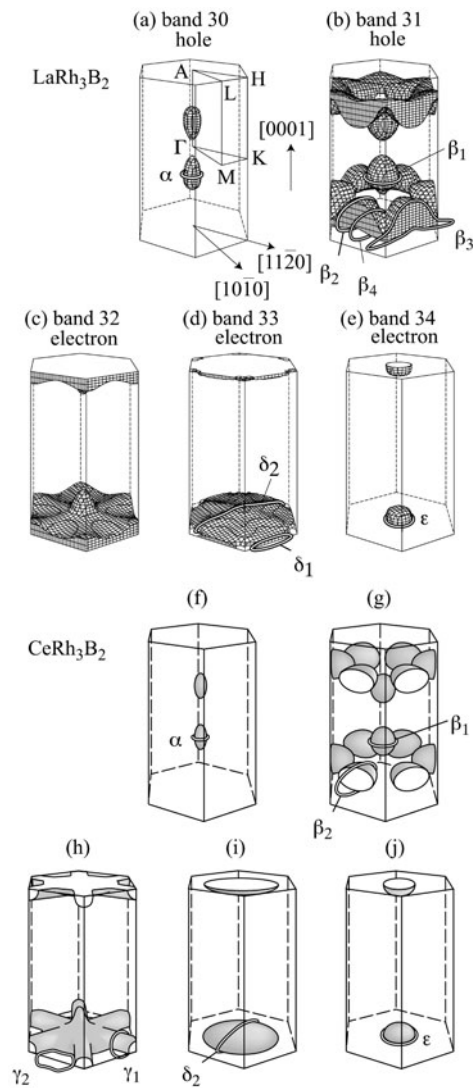


Figure 4. (a)–(e) Theoretical Fermi surfaces in LaRh_3B_2 , and (f)–(j) Fermi surfaces obtained experimentally in CeRh_3B_2 .

On the basis of these Fermi surfaces in LaRh_3B_2 , we simply constructed the corresponding Fermi surfaces for CeRh_3B_2 , which are shown in figures 4(f)–(j), together with the thick solid curves in figure 2. Our analyses are as follows. Branches α , β_1 and ϵ are in principle unchanged between LaRh_3B_2 and CeRh_3B_2 , although the volume of the each Fermi surface is slightly changed. The connected band 31-hole Fermi surfaces named β_2 , β_3 and β_4 of LaRh_3B_2 in figure 4(b) are separated into three ellipsoidal Fermi surfaces in CeRh_3B_2 . The flat quasi-one-dimensional band 33-electron Fermi surface of LaRh_3B_2 is changed into a flat ellipsoidal closed Fermi surface in CeRh_3B_2 . The quasi-one-dimensional band 32-electron Fermi surface of LaRh_3B_2 is also changed into a multiply connected Fermi surface with arms named γ_1 along $[11\bar{2}0]$. The volume of hole Fermi surfaces in CeRh_3B_2 is as follows: $0.002 V_{\text{BZ}}$ for branch α , $0.012 V_{\text{BZ}}$ for two branches β_1 and $0.105 V_{\text{BZ}}$ for these branches β_2 , indicating a total volume

of $0.12 V_{\text{BZ}}$ for the hole Fermi surfaces, where V_{BZ} is the volume of the Brillouin zone. The corresponding compensated electron Fermi surfaces are $0.008 V_{\text{BZ}}$ for branch ε and $0.039 V_{\text{BZ}}$ for branch δ_2 . A remaining volume of $0.07 V_{\text{BZ}}$ is expected for the band 32-electron Fermi surface and is shown in figure 4(h). CeRh_3B_2 is also a compensated metal.

The present analysis is in principle based on the 4f localized model. The contribution of the 4f localized electron to the volume of the Fermi surface is thus small. Even in the localized system, however, the presence of the 4f electron alters the Fermi surface through the 4f electron contribution to the crystal potential and through the introduction of magnetic Brillouin zone boundaries and magnetic energy gaps which occur when the 4f electron moments order. We note that the Fermi surfaces with up- and down-spin states are not observed, apart from a small Fermi surface named α . This is mainly due to a small ordered moment of $0.4 \mu_{\text{B}}/\text{Ce}$.

The electronic specific heat coefficient in CeRh_3B_2 is approximately estimated from the cyclotron mass: $0.27 \text{ mJ K}^{-2} \text{ mol}^{-1}$ for branch α ($m_{\text{c}}^* = 0.33 m_0$ and $0.37 m_0$ for $H \parallel [0001]$), $0.55 \text{ mJ K}^{-2} \text{ mol}^{-1}$ for two branches β_1 ($m_{\text{c}}^* = 0.60 m_0$ for $H \parallel [0001]$), $8.67 \text{ mJ K}^{-2} \text{ mol}^{-1}$ for three branches β_2 ($m_{\text{c}}^* = 2.0 m_0$ for $H \parallel [0001]$ and $1.9 m_0$ for $H \parallel [10\bar{1}0]$), $2.7 \text{ mJ K}^{-2} \text{ mol}^{-1}$ for branch δ_2 ($m_{\text{c}}^* = 2.4 m_0$ for $H \parallel [10\bar{1}0]$), and $1.1 \text{ mJ K}^{-2} \text{ mol}^{-1}$ for branch ε ($m_{\text{c}}^* = 2.3 m_0$ for $H \parallel [0001]$ and $1.7 m_0$ for $H \parallel [10\bar{1}0]$), indicating a total of about $13 \text{ mJ K}^{-2} \text{ mol}^{-1}$. The electronic specific heat coefficient of CeRh_3B_2 is reported as 16 and $20 \text{ mJ K}^{-2} \text{ mol}^{-1}$ [5, 19], while our specific heat measurement indicated $18 \text{ mJ K}^{-2} \text{ mol}^{-1}$. The remaining band 32-electron Fermi surface, shown in figure 4(h), is thus expected to possess about $5 \text{ mJ K}^{-2} \text{ mol}^{-1}$, approximately reasonable from the volume of its Fermi surface. These results indicate that the present Fermi surfaces shown in figures 4(f)–(j) are complete and there exist no other large Fermi surfaces in CeRh_3B_2 . CeRh_3B_2 is thus not a heavy fermion compound. This is most likely due to an extremely high ordered temperature and the nature of almost localized 4f electrons.

Quite recently ferromagnetism was theoretically discussed on the basis of a two-band model of which the basic ingredient is an uncorrelated dispersive band (mainly Rh 4d orbitals) hybridized with a correlated and narrow 4f band [15]. It is not clear whether this theory is applied to CeRh_3B_2 or not. From the present dHvA results, it is important to consider that the contribution of the 4f electron to the volume of the Fermi surface is small because the topology of the Fermi surface in CeRh_3B_2 is very similar to that of LaRh_3B_2 , although the total volume of the Fermi surface in CeRh_3B_2 is slightly smaller than that of LaRh_3B_2 and each Fermi surface is slightly different between two compounds.

The short distance of the lattice constant along $[0001]$ is found to be reflected as wavy but flat Fermi surfaces in the basal plane, which is mainly due to a well-hybridized band of Rh 4d and B 2p electrons. Observation of these unique Fermi surfaces with a quasi-one-dimensional character is the first such case in a rare earth compound. This might be related to the origin of the high Curie temperature, together with the hybridization effect between the conduction electrons and almost localized 4f electrons.

We are grateful to Professor Y Kuramoto for helpful discussion. This work was supported by the Grant-in-Aid for COE Research (10CE2004) of the Ministry of Education, Culture, Sports, Science and Technology.

References

- [1] Ōnuki Y, Goto T and Kasuya T 1991 *Materials Science and Technology* vol 3A, ed K H J Buschow (Weinheim: VCH) p 545
- [2] Ōnuki Y, Inada Y, Ohkuni H, Settai R, Kimura N, Aoki H, Haga Y and Yamamoto E 2000 *Physica B* **280** 276
- [3] Dhar S K, Malik S K and Vijayaraghavan R 1981 *J. Phys. C: Solid State Phys.* **14** L321

- [4] Malik S K, Vijayaraghavan R, Wallace W E and Dhar S K 1983 *J. Magn. Magn. Mater.* **37** 303
- [5] Yang K N, Torikachvili M S, Maple M B and Ku H C 1984 *J. Low Temp. Phys.* **56** 601
- [6] Kasaya M, Okabe A, Takahashi T, Satoh T and Kasuya T 1988 *J. Magn. Magn. Mater.* **76/77** 347
- [7] Ku H C, Meisner G P, Acker F and Johnston D C 1980 *Solid State Commun.* **35** 91
- [8] Langen J, Jackel G, Schlabit W, Veit M and Wohlleben D 1987 *Solid State Commun.* **64** 169
- [9] Misemer D K, Auluck S, Kobayashi S I and Harmon B N 1984 *Solid State Commun.* **52** 955
- [10] Kitaoka Y, Kishimoto Y, Asayama K, Kohara T, Takeda T, Vijayaraghavan R, Malik S K, Dhar S K and Rambabu D 1985 *J. Magn. Magn. Mater.* **52** 449
- [11] Fujimori A, Takahashi T, Okabe A, Kasuya M and Kasuya T 1990 *Phys. Rev. B* **41** 6783
- [12] Schillé J Ph, Bertran F, Finazzi M, Brouder Ch, Kappler J P and Krill G 1994 *Phys. Rev. B* **50** 2985
- [13] Shaheen S A, Schilling J S and Shelton R N 1985 *Phys. Rev. B* **31** 656
- [14] Alonso J A, Boucherle J X, Givord F, Schweizer J, Gillon B and Lejay P 1998 *J. Magn. Magn. Mater.* **177–181** 1048
- [15] Batista C D, Bonča J and Gubernatis J E 2002 *Phys. Rev. Lett.* **88** 187203
- [16] Harima H, Sakai O, Kasuya T and Yanase A 1988 *Solid State Commun.* **66** 603
- [17] Ebihara T, Inada Y, Murakawa M, Uji S, Terakura C, Terashima T, Yamamoto E, Haga Y, Ōnuki Y and Harima H 2000 *J. Phys. Soc. Japan* **69** 895
- [18] Harima H and Takegahara K 2003 in preparation
- [19] Shaheen S A, Shilling J S, Klavins P, Vining C B and Shelton R N 1985 *J. Magn. Magn. Mater.* **47/48** 285